**Electronic Supplementary Information**

# Cancer cell targeting and therapeutic delivery of silver nanoparticles by mesoporous silica nanocarriers: insights into the action mechanisms by quantitative proteomics

Sandra Montalvo-Quirós[a,b], Guillermo Aragoneses-Cazorla[a], Laura Garcia-Alcalde[a], María Vallet-Regí[c,d], Blanca González[c,d,*], Jose L. Luque-García[a,*]

[a] Departamento de Química Analítica, Facultad de Química, Universidad Complutense de Madrid, Avenida Complutense s/n, 28040 Madrid, Spain

[b] Centro de Estudios Tecnológicos y Sociales, Universidad Francisco de Vitoria, 28223, Pozuelo de Alarcón Madrid, Spain

[c] Departamento de Química en Ciencias Farmacéuticas, Facultad de Farmacia, Universidad Complutense de Madrid, Instituto de Investigación Sanitaria Hospital 12 de Octubre (imas12), Plaza Ramón y Cajal s/n, 28040 Madrid, Spain

[d] Centro de Investigación Biomédica en Red de Bioingeniería, Biomateriales y Nanomedicina (CIBER-BBN), Spain

* Corresponding authors: jlluque@ucm.es (J.L. Luque-Garcia); blancaortiz@ucm.es (B. González)

## Electronic Supplementary Information Summary

Characterization techniques; Synthesis of **MSNs** and **MSNs-COOH$_{ext}$** materials; TEM, SEM and DRX characterization of MSN materials (Figure SI.1); Hydrodynamic diameter distribution obtained by DLS for the **MSNs-Tf-AgNPs** material (Figure SI.2); $^{13}C\{^{1}H\}$ NMR spectrum of BSA (Figure SI.3); $N_2$ adsorption isotherms and pore diameters and $N_2$ adsorption disscusion (Figure SI.4); TEM images of M**SNs-BSA-AgNPs** and **MSNs-Tf-AgNPs** materials (Figure SI.5); TEM images of silver nanoclusters (Figure SI.6); internalization assay of **MSNs** and **MSNs-Tf-AgNPs** inside HepG2 and MC3T3-E1 cells (Figure SI.7); cell viability assay of HepG2 cells exposed to **MSNs** and **MSNs-Tf-AgNPs** (Figure SI.8); TEM images of ultrathin sections of HepG2 cells exposed to **MSNs-Tf-AgNPs** (Figure SI.9); SILAC experiment (Figure SI.10).

## Characterization techniques

Thermogravimetric analysis (TGA) and differential thermal analysis (DTA) were performed in a Perkin Elmer Pyris Diamond TG/DTA analyser (Perkin Elmer, California, USA) by placing approximately 5 mg of sample in an aluminium crucible and applying 5 °C/min heating ramps from room temperature to 600 °C under a flow rate of 100 mL/min of air. Chemical microanalyses were performed with a Perkin Elmer 2400 CHN and a LECO CHNS-932 thermoanalyzers.

Solid state magic angle spinning nuclear magnetic resonance (MAS NMR) and cross polarization magic angle spinning nuclear magnetic resonance (CP MAS NMR) spectra were obtained on a Bruker Avance AV-400WB spectrometer equipped with a solid state probe using a 4 mm zirconia rotor. Typical measurement conditions were as follows: $^{13}C$ NMR experiments were conducted with proton decoupling, the spectrometer frequency was set to 100.62 MHz ($^{13}C$) and 400.13 MHz ($^{1}H$) and MAS rotation rate was maintained at 6 kHz. The NMR spectra consisted of 15000 to 17500 acquisitions with cross-polarization contact times of 2 ms, 2.5 μs pulse wide and a 5 s recycle delay. Chemical shift values were referenced at 176.1 ppm to carbonyl carbon of glycine. $^{29}Si$ NMR quantitative spectra were obtained at 79.49 MHz with MAS rotation rate of 12 kHz, a pulse wide of 4.5 μs, a recycle delay of 5 s, and the number of scans was 17000 to 20000. $^{29}Si$ CP MAS NMR experiments were done setting the transmitter frequency to 79.49 MHz ($^{29}Si$) and 400.13 MHz ($^{1}H$), samples were spun to 12 kHz and a 5 s recycle delay, a 4.5 μs pulse wide and a cross-polarization contact time of 3.5 ms were employed. All chemical shift values reported were externally referenced at 0 ppm to 3-(trimethylsilyl)-1-propanesulfonic acid sodium salt (DSS sodium salt).

The powder X-ray diffraction (XRD) measurements were performed in a Philips X'Pert diffractometer with Bragg-Brentano geometry operating with Cu Kα radiation (wavelength 1.5406 Å) at 40 kV and 20 mA (Philips Electronics NV, Eindhoven, Netherlands). Low-angle XRD patterns were collected in the 2θ range between 0.6° and 8° with a step size of 0.02° and contact time of 5 s per step.

The textural properties of the materials were determined by $N_2$ adsorption porosimetry by using a Micromeritics ASAP 2020 (Micromeritics Co., Norcross, USA). To perform the $N_2$ measurements, *ca.* 30 mg of each sample was previously degassed under vacuum for 24 h at 40 °C. The surface area ($S_{BET}$) was determined using the Brunauer-Emmett-Teller (BET) method and the pore volume ($V_P$) was estimated from the amount of $N_2$ adsorbed at a relative pressure of 0.98. The pore size distribution between 0.5 and 40 nm was calculated from the desorption branch of the isotherm by means of the Barrett-Joyner-Halenda (BJH) method and the average mesopore size ($D_p$) was determined from the maximum of the pore size distribution curve.

Electrophoretic mobility measurements of the materials suspended in water were used to calculate the zeta-potential (ζ) values of the nanoparticles. Measurements were performed in a Zetasizer Nano ZS (Malvern Instruments Ltd., United Kingdom) equipped with a 633 nm "red" laser. For this purpose, 1 mg of nanoparticles was added to 10 mL of water followed by vortex and ultrasound to get a homogeneous suspension. Measurements were recorded by placing *ca.* 1 mL of suspension in DTS1070 disposable folded capillary cells (Malvern Instruments). The hydrodynamic size of nanoparticles was measured by dynamic

light scattering (DLS) with the same Malvern instrument. Values presented are mean ± SD from triplicate measurements.

Surface morphology was analysed by scanning electron microscopy (SEM) on a JEOL JSM 6335F microscope. For this purpose, samples were mounted onto a copper stud, dried at 70 °C for 48 h under vacuum and coated with a film of Au previous to observation.

Transmission Electron Microscopy (TEM) and energy dispersive X-ray spectroscopy were carried out with a JEOL JEM 1400 or 2100 instruments operated at 120 and 200 kV, respectively (JEOL Ltd., Tokyo, Japan). Sample preparation was performed by dispersing *ca.* 1 mg of sample in 1 mL of 1-butanol followed by sonication in a low power bath sonicator (Selecta, Spain) for 5 min and then depositing one drop of the suspension onto carbon-coated copper grids.

## Reagents and equipment

Fluorescein isothiocynate (FITC), tetraethylorthosilicate (TEOS), cetyltrimethylammonium bromide (CTAB), N-(3-dimethylaminopropyl)-N'-ethylcarbodiimide hydrochloride (EDC.HCl), 2-morpholinoethanesulfonic acid (MES), bovine serum albumin (BSA), transferrin human (Tf), citric acid, silver nitrate 99.9% and water (HPLC grade) were purchased from Sigma-Aldrich. 3-Aminopropyltriethoxysilane 97% (APTS), 3-(triethoxysilyl)propylsuccinic anhydride 94% (TESPSA) were purchased from ABCR GmbH & Co.KG. All other chemicals (ammonium nitrate, absolute EtOH, dry toluene, NaOH, etc.) were of the highest quality commercially available and used as received.

## Materials synthesis

**MSNs.** Under $N_2$ atmosphere, APTS (5 μL, 0.023 mmol) was added over a stirred FITC (2 mg, 0.005 mmol) solution in EtOH (0.5 mL). The reaction mixture was stirred at RT for 2 h in the dark and then added to a mixture of EtOH (1 mL) and TEOS (5 mL, 23 mmol). This solution was subsequently placed on a syringe dispenser to be transferred to the next reaction. The cationic surfactant CTAB (1 g, 2.74 mmol) was dissolved in 480 mL of water with 3.75 mL of NaOH 2 M and the solution was heated to 80 °C. Then, the solution containing TEOS and the silane-modified fluorescein was slowly added at a constant rate of 0.43 mL/min under vigorous stirring. The reaction was vigorously stirred for 1 h at 80 °C in the dark and then the suspension was cooled to room temperature, centrifuged at 11000 rpm for 20 min and the particles washed several times with water, EtOH and finally dried.

**MSNs-COOH$_{ext}$.** For the external surface functionalization of MSNs with –COOH groups, pore surfactant containing material was employed and, therefore, approximately a quarter of the specific surface area of the

free-surfactant material (1054.92 $m^2/g$) was considered to be functionalized. Prior to surface functionalization 1 g of CTAB-containing MSNs (40% wt., *i.e.*, 0.6 g MSNs) was dehydrated at 80 °C, under vacuum for 3 h in the dark, and subsequently re-dispersed under an inert atmosphere in dry toluene (58 mL). A solution of TESPSA (145 mg, 10% exc.) in 15 mL of dry toluene was added to the vigorously stirred suspension of the CTAB-containing MSNs and the mixture was heated to 110 °C overnight in the dark. The reaction mixture was centrifuged at 14000 rpm for 15 min and the obtained solid was exhaustively washed with toluene and acetone and finally dried. The surfactant was removed from the functionalized material by heating a well dispersed suspension of the obtained solid in EtOH (360 mL), water (40 mL) and HCl (10 mL) overnight at 60 °C and then the solid was washed with water and EtOH. This extraction process was repeated for 2 h and the solid dried under vacuum. The nominal or theoretical value of –COOH groups in this material was $1.22 \times 10^{-3}$ mol/g $SiO_2$.

**Synthesis and characterization of MSNs and MSNs-$COOH_{ext}$**

Fluorescent MSNs were prepared following a modified Stöber method in which the fluorescent dye was covalently linked to the silica network [1,2,3]. SEM analysis revealed that the obtained MSNs had uniform spherical shape with an average particle diameter of *ca.* 150 nm, and TEM images showed a highly ordered mesostructure of the MSNs. Low-angle XRD measurement showed a well-resolved pattern indexed to a *p6mm* symmetry of 2D hexagonal MCM-41 materials with a unit cell parameter of 4.54 nm (Figure SI.1). The well-ordered mesoporous structure was also confirmed by $N_2$ adsorption porosimetry, possessing an average pore diameter of 2.80 nm and 1054.9 $m^2/g$ of surface area (Figure SI.2).

To provide anchoring points for the proteins, the external surface of the MSNs was functionalized with carboxylic acid groups in a first step, using a post-synthesis method [1]. The condensation of the succinic anhydride alkoxysilane derivative TESPSA with the silanol groups of the outer silica surface, under water free conditions [4], was performed using the as-synthesized MSN material containing the organic template filling the pores. With this methodology, a favoured functionalization of the outer surface of MSNs is foreseeable [5]. The surfactant was removed afterwards using acidified ethanol as extracting solution,

[1] A. Martínez, E. Fuentes-Paniagua, A. Baeza, J. Sánchez-Nieves, M. Cicuéndez, R. Gómez, F. J. de la Mata, B. González and M. Vallet-Regí, *Chem. Eur. J.*, 2015, **21**, 15651-15666. Mesoporous Silica Nanoparticles Decorated with Carbosilane Dendrons as New Non-viral Oligonucleotide Delivery Carriers.

[2] V. Y.-S. Lin, C.-P. Tsai, H.-Y. Huang, C.-T. Kuo, Y. Hung, D.-M. Huang, Y.-C. Chen and C.-Y. Mou, *Chem. Mater.*, 2005, **17**, 4570-4573. Well-ordered Mesoporous Silica Nanoparticles as Cell Markers.

[3] M. Grün, I. Lauer and K. K. Unger, *Adv. Mater.*, 1997, **9**, 254-257. The Synthesis of Micrometer- and Submicrometer-Size Spheres of Ordered Mesoporous Oxide MCM-41.

[4] M. Lim and A. Stein, *Chem. Mater.*, 1999, **11**, 3285-3295. Comparative Studies of Grafting and Direct Syntheses of Inorganic-Organic Hybrid Mesoporous Materials.

[5] F. de Juan and E. Ruiz-Hitzky, *Adv. Mater.*, 2000, **12**, 430-432. Selective Functionalization of Mesoporous Silica.

affording in the same stage the anhydride ring opening. The required amount of alkoxysilane derivative was calculated to achieve a maximum coverage of the external nanoparticle surface (a 100% nominal degree of functionalization). For this, approximately a quarter of the specific surface area was estimated to correspond to the external surface and a molar ratio of three Si-OH groups with one R-Si(OEt)$_3$ molecule was the stoichiometry used. In addition, it was presumed that the average surface concentration of Si-OH in silica materials is 4.9 OH/nm$^2$ [6].

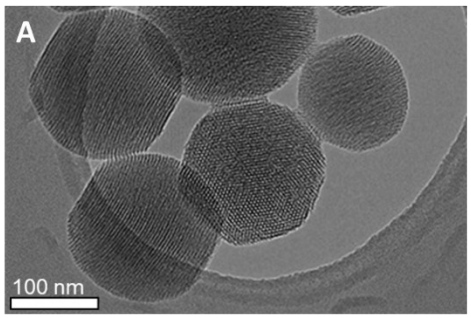


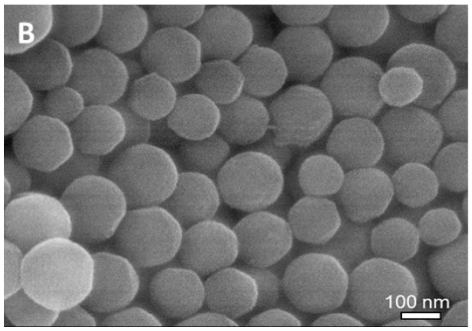


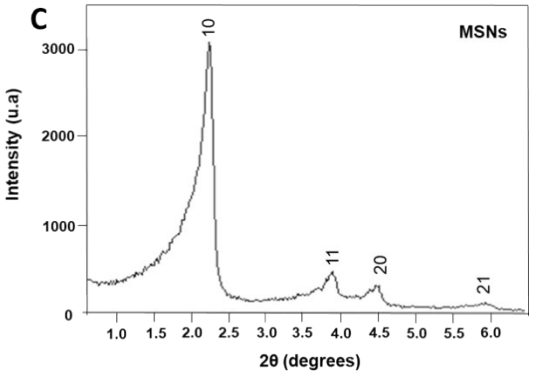


D

| (*hk*) | 2θ | $d_{hk}$ (nm) |
|---|---|---|
| 10 | 2.24 | 3.935 |
| 11 | 3.9 | 2.263 |
| 20 | 4.5 | 1.958 |
| 21 | 5.96 | 1.480 |

**Figure SI.1.** TEM (A) and SEM (B) images of the surfactant extracted **MSNs** material. Low angle powder X-ray diffraction pattern of the starting mesoporous material **MSNs** (C). Table of DRX maxima and lattice spacing ($d_{hk}$) of **MSNs** (D).

[6] L. T. Zhuravlev, *Colloids Surfaces A Physicochem. Eng. Asp.*, 2000, **173**, 1-38. The Surface Chemistry of Amorphous Silica. Zhuravlev Model.

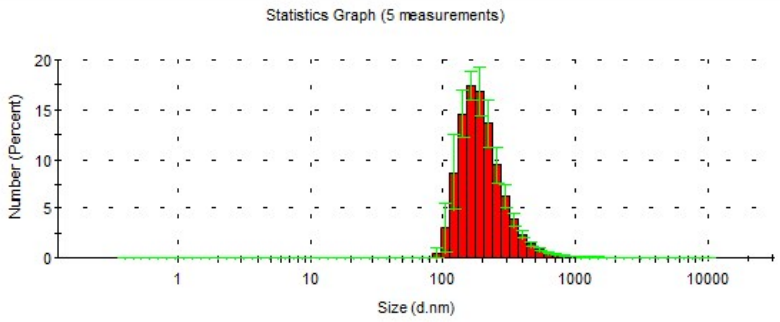


**Figure SI.2.** Hydrodynamic diameter distribution obtained by DLS for the **MSNs-Tf-AgNPs** material

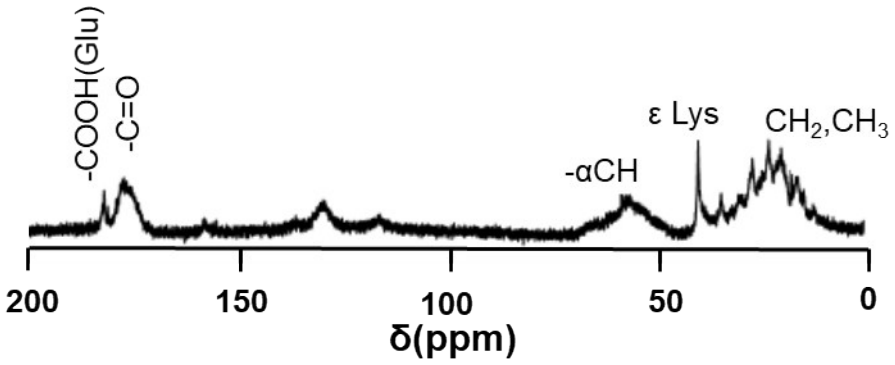


**Figure SI.3.** $^{13}C\{^{1}H\}$ NMR spectrum of BSA, in $D_2O$ (330 mg/mL). Assignments based on reference *Nicolau Beckmann, Carbon-13 NMR Spectroscopy of Biological Systems, Academic Press (1995).*

A

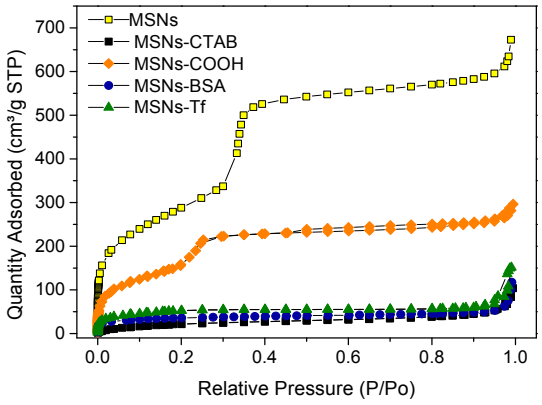


B

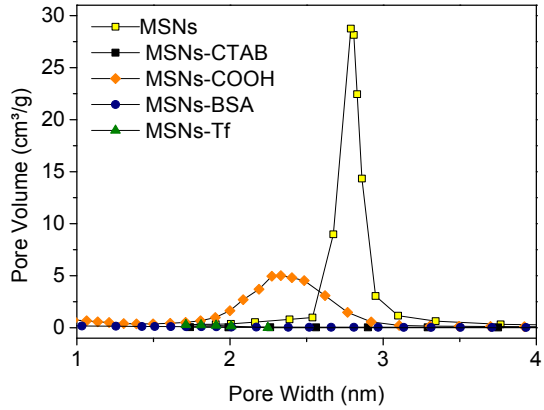


C

| Material | $S_{BET}$ ($m^2$/g) | $D_p$ (nm) | $V_T$ ($cm^3$/g) | $V_P$ ($cm^3$/g) |
|---|---|---|---|---|
| **MSNs** | 1054.9 | 2.80 | 0.946 | 0.854 |
| **MSNs-CTAB** | 90.9 | - | - | - |
| **MSNs-COOH$_{ext}$** | 649.8 | 2.30 | 0.409 | 0.255 |
| **MSNs-BSA** | 122.6 | 1.30 | 0.181 | 0.102 |
| **MSNs-Tf** | 189.0 | 1.70 | 0.131 | 0.085 |

**Figure SI.4.** $N_2$ adsorption isotherms of the MSN materials, before and after functionalisation with carboxylic acid groups and proteins (A). Pore-size distributions for the mesoporous samples (B). Textural parameters of the MSN materials obtained by $N_2$ adsorption measurements (C), where $S_{BET}$ is the specific surface area obtained by using the BET equation, $D_P$ is the pore diameter calculated by using the BJH method, $V_t$ is the total pore volume obtained at $P/P_0$=0.99 and $V_P$ is the total pore volume obtained at $P/P_0$ = 0.60.

The physical properties of these mesoporous silica nanoparticles were analyzed by $N_2$ adsorption-desorption measurements (Figure SI.2). As expected, **MSNs-CTAB** showed a characteristic isotherm of a nonporous material, possessing a very small surface area (90.88 $m^2$/g). After removal the surfactant and the functionalization with acids groups, **MSNs-COOH$_{ext}$** showed high surface area (649.79 $m^2$/g) and large pore volume (0.409 $cm^3$/g). These values were lower that the initial extracted material without functionalization, confirming the carboxylic acids grafting. This extracted material exhibited the characteristic type IV BET isotherm, verifying the presence of a cylindrical, one-dimensional channel-like mesoporous structure in the nanoparticles. After proteins were covalently linked onto external surface of the nanoparticles, the surface area and the pore volume, in both cases, were greatly reduced due to the partially blocking of the pores entrances.

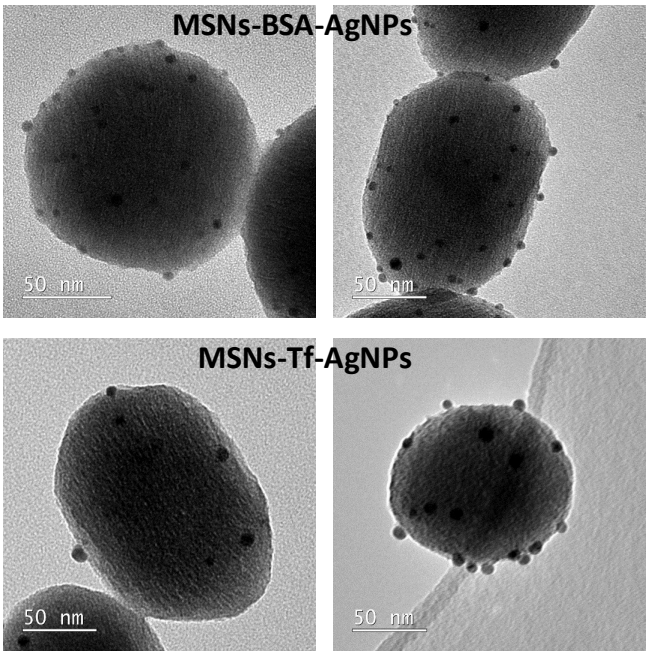


**Figure SI.5.** TEM images of M**SNs-BSA-AgNPs** (upper row) and **MSNs-Tf-AgNPs** (lower row) materials.

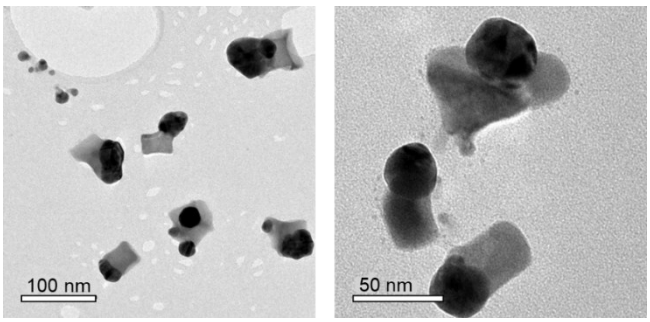


**Figure SI.6.** TEM images of silver nanoclusters obtained by using the free transferrin protein as template.

**Nucleation of silver on transferrin.** 1 mg of transferrin was dissolved in 2 mL of HEPES buffer 20 mM (pH 8.2). Then, 100 μL of $AgNO_3$ (10 mM) was added over the transferrin solution. The reaction mixture was stirred for 12 h at room temperature in the dark. Finally, a yellow-orange precipitate was obtained.

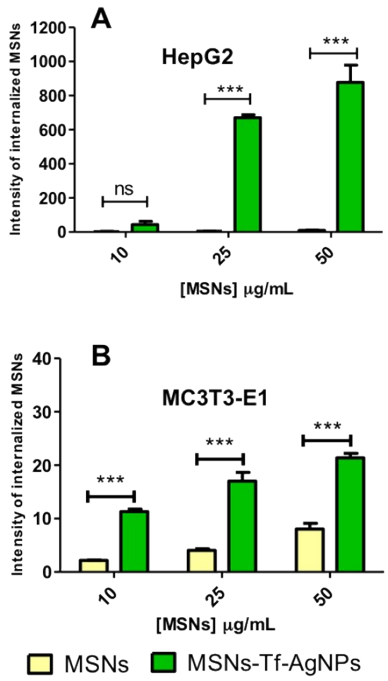


**Figure SI.7.** Internalization of MSNs materials inside HepG2 (A) and MC3T3-E1 (B) cells exposed to different concentrations (10, 25, 50 μg/mL) of **MSNs** and **MSNs-Tf-AgNPs** during 24 (n = 3). Statistical significance: ***p < 0.001. ns: not significant.

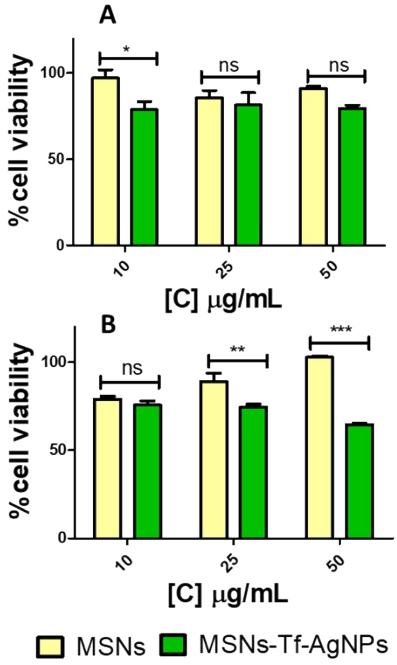


**Figure SI.8.** Cell viability assay at 24 h (A) and 48 h (B) of HepG2 cells exposed to different concentrations (10, 25, 50 μg/mL) of **MSNs** and **MSNs-Tf-AgNPs**. Data were analyzed by ANOVA followed by Bonferroni´s multiple-comparison test. Statistical significance: *p < 0.05, **p <0.01, ***p < 0.001.

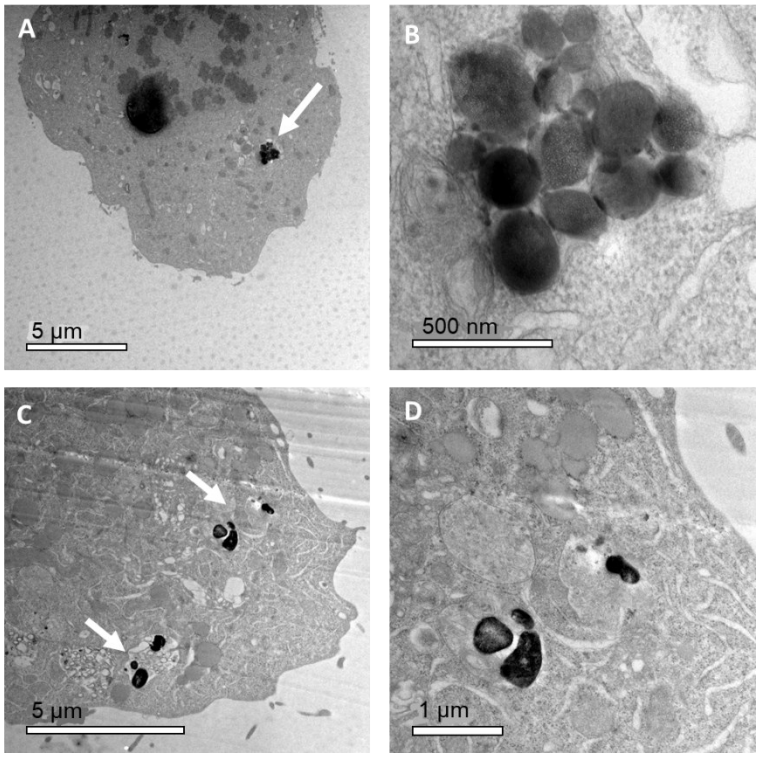


**Figure SI.9.** TEM micrographs of ultrathin sections of HepG2 cells exposed to 25 μg/mL of **MSNs-Tf-AgNPs** for 24 h. HepG2 cell in cellular division progress showing internalized nanoparticles (A and B). A section of HepG2 cell with different groups of nanoparticles (C and D).

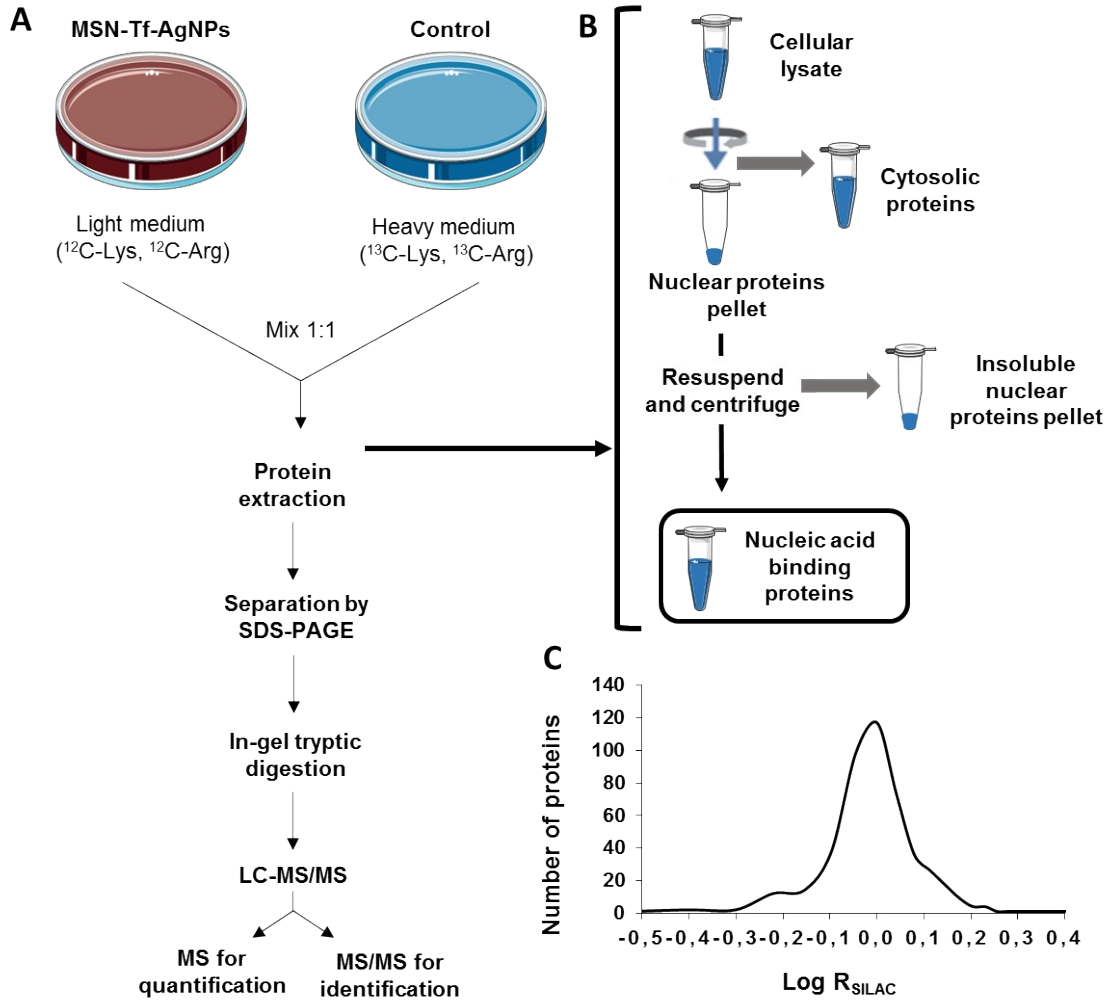


**Figure SI.10.** SILAC experiment. A) General scheme of the SILAC experiment. B) Nuclear protein extraction procedure. C) Distribution of the SILAC ratios for the identified proteins. Most quantified proteins presented a SILAC ratio close to 1, as expected for a 1:1 mixture.